

Variation In Wave Steepness and Wave Age-A Case Study in The Arabian Sea from Buoy Measurements During Post-Monsoon

Kalyani M^{1,*}, Vengatesan G², Sridharan R², Biswajit H³, Jossia Josph K⁴, Arul Muthuiah M⁵

Commented [s1]: <Author> Please Check Affiliation

Abstract

The National Institute of Ocean Technology (NIOT) moored buoy measurements in the Central Arabian Sea (AS) at AD07 location (68.87 E, 15.07 N) during the year 2015 are utilized to understand wind and wave growth characteristics at this location during the post-monsoon season covering the three-month period from October to December (OND). The wave direction followed the wind from Northeast while the swells were predominantly from the Southern Indian Ocean (SIO) from distant storms. This season is characterized by low to medium wind and wave conditions with the peak period (T_p) exhibiting two distinct peaks in sea and swell ranges. The wave age and wave steepness are evaluated from the data which are important to understand the wind-wave growth with energy balance equation of significant waves. The buoy algorithm separates sea and swell at 10 s, and hence, the results are presented for the two cases for T_p less than 10s (wind sea range) and for T_p more than 10 s (swell range). It is found that 32.5 % are old swells, 6.7 %, are mature swells, 46.6 % are young swells and only 14.3 % are wind seas at AD07 during post-monsoon season. As there were no cyclones that influenced AD07 during this period (Chapala & Megh were away from AD07 and had landfall on Gulf coast, no impact at AD07) the swells predominantly are from the SIO. In addition, the available empirical relationship on wave steepness and wave age based on the 3/2 power law for wind seas is compared for the present study and found to follow the trend. A new coefficient is derived for AD07 location in the unobstructed deep waters for post-monsoon season. The empirical relationship developed between the non-dimensional wave height and wave period in the shallow waters of AS is compared with present data. A similar relationship with modified coefficient for deep waters is derived AD07 in the central AS for post-monsoon season.

Keywords: Buoy, Arabian sea, post-monsoon, wave steepness; wave age, empirical relationship

*Author for Correspondence

Kalyani M
E-mail: kalyani.niot@gmail.com

¹Scientist-E, Ocean Observation Systems Group, National Institute of Ocean Technology, Chennai, India

²Scientific Officer Grade II, Ocean Observation Systems Group, National Institute of Ocean Technology, Chennai, India

³Scientist-D, Ocean Observation Systems Group, National Institute of Ocean Technology, Chennai, India

⁴Scientist-F, Ocean Observation Systems Group, National Institute of Ocean Technology, Chennai, India

⁵Group Head in Charge, Ocean Observation Systems Group, National Institute of Ocean Technology, Chennai, India

Received Date: March 27, 2025

Accepted Date: April 04, 2025

Published Date: April 07, 2025

Citation: Kalyani M, Vengatesan G, Sridharan R, Biswajit H, Jossia Josph K, Arul Muthuiah M. Variation in Wave Steepness and Wave Age-A Case Study in the Arabian Sea from Buoy Measurements during Post-Monsoon. Journal of Offshore Structure and Technology. 2025; 12(2): 10–21p.

INTRODUCTION

Arabian sea is characterized by swells during the entire year. During pre and post monsoon, seas and swells are distinctly separated by two peaks while during the monsoon generally mixed seas exist. Wave steepness is used as a measure estimate the separation frequency of wind sea and swell. Swell decay rate is related to a reverse momentum flux process and influences the marine atmospheric boundary layer. Sanil Kumar et. at (2010) found that even with low wind speeds of less than 3 m/s, significant wave height more than 2m is present due to the swells in the Arabian Sea, during the onset of summer monsoon off Goa in 14 m water depth

during 2006 and the waves are found to be predominantly (67%) swells with young seas [12]. Aboobacker et al. (2011b) have identified potential swell generation areas during different seasons in the Arabian Sea (from SW direction during SW monsoon and from SW/SSW and NW directions during both pre-monsoon and post-monsoon seasons). An attempt has been made to understand the co-existence of wind seas and swells at different coastal regions in the Indian side of the Arabian Sea during non-monsoon season by Rashmi et al. (2013) [11]. The link between North Indian Ocean (NIO) high swell events and the meteorological conditions over the Southern Indian Ocean (SIO) is explored, using a combination of in situ measurements and model simulations for the year 2005 by Remya et al. (2016) [10].

The above studies in the Arabian Sea are mostly pertaining to coastal locations where the wave height and direction transform based on the bathymetric contours and coastline orientation with sea-land breeze effects. Whereas the present paper deals with wave growth in the deep waters with continuous supply of wind and is unobstructed by the bathymetry. These studies cover different years and different seasons with less emphasis given to post-monsoon characteristics in deep waters. Hence, the present study focuses on the wind wave characteristics with reference to the wave age and wave steepness at AD07 in deep waters of AS in 2015.

The development of pure wind-driven waves in deep waters is controlled by three basic processes: energy input from wind to surface waves, nonlinear wave-wave energy transfer and energy dissipation due to wave breaking. Numerical wave models are developed based on wind wave theory to study the wind-wave growth with an energy balance equation for significant wave, for which a relationship between wave steepness ϵ and wave age β , is needed. Various ϵ - β relationships have been proposed on the basis of both observations and physical simulations. However, a considerable discrepancy still exists among these proposed relationships. In addition, both wave steepness and wave age can be used to discriminate wind waves from swells, since wind waves are typically steeper and younger than swells. Thus, the ϵ - β relationship is still an important issue in wind wave study.

In earlier proposed ϵ - β relationships, it is assumed that wave steepness is dependent on wave age only [17,18]. Wang (1990) and Guan and Sun (2002) obtained a ϵ - β relationship based on the “3/2-power law” proposed by Toba (1972), in which a drag coefficient is assumed to be constant [6,15]. Drag coefficient is dependent on wind speed and is mostly parameterized as a linear function of wind speed [3] [13] [7] [4] [20]. Guan and Xie (2004) proposed that the drag coefficient is a nearly-linear function of wind speed with the slope dominated by wave steepness [5]. Hou and Wang (1993) presented a relationship based on the wave spectrum width while Wu et al. (1980) proposed based on a non-dimensional fetch, but only a steady wind blowing for a sufficiently long duration is the fetch definite, which is rare in field experiment [7,19]. Thus, it is more practical to establish a ϵ - β relationship to reconcile the discrepancy mentioned above, in which an effective parameter is included instead of nondimensional fetch.

In order to interpret the discrepancy among the existing ϵ - β relationships, in this paper, observations of both wind and waves from moored buoy at AD07 location are utilized in deriving the empirical relationship for various ranges of wind seas and swells during post-monsoon season which will help in guiding the numerical models as well as laboratory physical model studies. Hence, the present paper finds its significance in deriving the empirical relationships between wave steepness and wave age as well as between wave height and peak period for wind seas. It also classifies the type of swells and quantifies them in the swell dominant conditions in the Arabian Sea.

METHODOLOGY

AD07 buoy is located at 68.87 E, 15.07 N in the central Arabian Sea on the west coast of India. During 2015 post-monsoon season two cyclones occurred (Chapala & Megh, Figure 1) during October and November but their tracks were far away from AD07, and their landfall was on the Gulf Coast and no impact was felt at AD07 location.

Not for Distribution, Uploading, or Publication on Any Other Website (or Online Platform)
Except Journals Official Website.

Galley Proof for Author's Review and Approval Only.

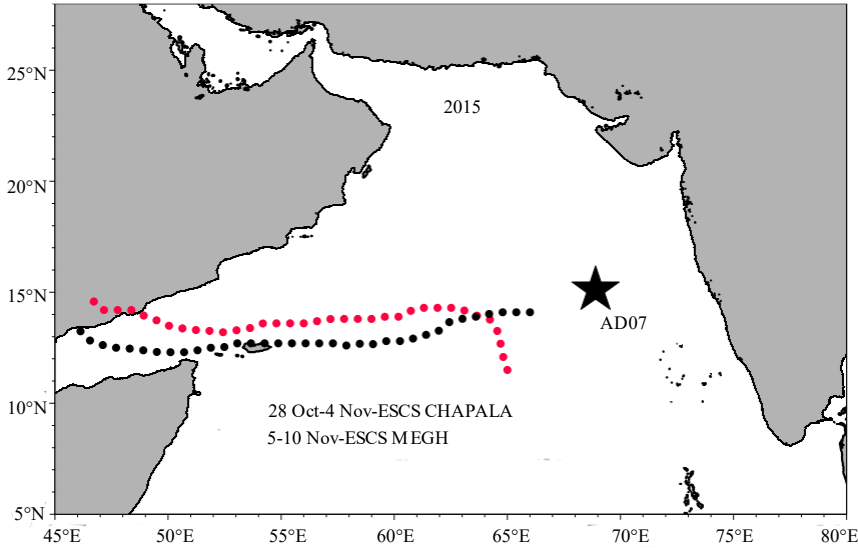


Figure 1 AD07 Buoy location with cyclone tracks during post-monsoon.

The buoy measurements on wind, wave parameters such as significant wave height (H_s), mean wave period (T_{m02}), Mean wave direction (MWD) along with peak period T_p are utilized in the study which are available at 3 hourly intervals. The buoy algorithm segregates sea and swell period at 10s cut off and the derived sea swell parameters are used. The timeseries of H_s and its sea and swell components are plotted in Figure 2 during the post-monsoon period OND 2015. Swells are observed throughout the period from 0.5 to 1.0 m height with maximum around 1.5 m during 1st week of October. Wind seas range between 0.5 to 2.0 m with maximum 2.5 m during the 2nd week of October.

The H_s -sea (wind seas) and H_s -sw (swell) are overlaid on T_p in Figure 3. Due to swell decay, the swell wave heights are smaller and wind-sea wave height due to local winds are higher. Whenever T_p is low and in wind-sea range (short period) it can be seen that the H_s -sea are higher.

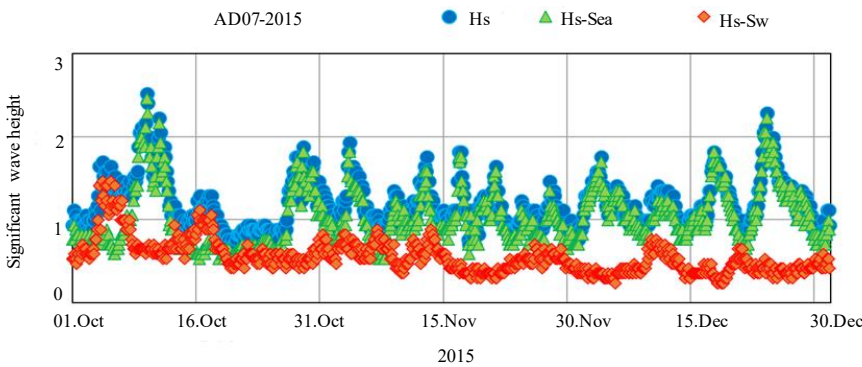


Figure 2 H_s and its components during post-monsoon 2015.

Not for Distribution, Uploading, or Publication on Any Other Website (or Online Platform) Except Journals Official Website.

Commented [s2]: <Author> Please Check Fig 1 TO 16 Text is Type

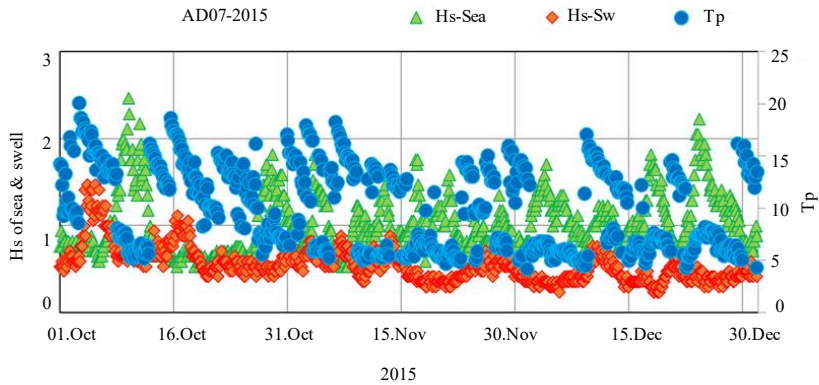


Figure 3. The sea & swell Hs are superposed on Tp during post-monsoon 2015.

The sea & swell mean wave periods are plotted along with Tp in Figure 4. Short periods below 10s are considered as sea range and long period waves above 10s are considered as swells. Pure wind seas (without swells) are present only for 14% of time and found to co-exist with the swells almost all the time during post-monsoon season.

During post-monsoon, local sea waves (MWD-Sea) are from Northeast direction in line with winds while the swell direction from SIO is from South as shown in Figure 5. Wind sea growth has been found while the swell propagates opposite to the direction of the wind and wind sea. The peak wave direction can be seen from both sea and swell directions depending on the peak is in the sea or swell range respectively.

Wind speed at 10 m height (U10) is plotted along with Tp in Fig. 6 (left panel). The variation of U10 with Tp is also shown in Fig. 6 (right panel). High wind speeds are observed for low Tp whereas, comparatively lesser U10 is observed for higher Tp. Accordingly, the Hs-sea is high and Hs-swell is less. Some data shows zero wind speed which are removed from analysis.

The components of Hs are plotted against the corresponding mean wave period for swells (left) and seas (right) in the Figure 7. It clearly indicates the demarcation of wave period at 10s. $T_{m02} < 10s$ as seas and $T_{m02} > 10s$ as swells. The wave heights of swells are mild and that of seas are relatively high.

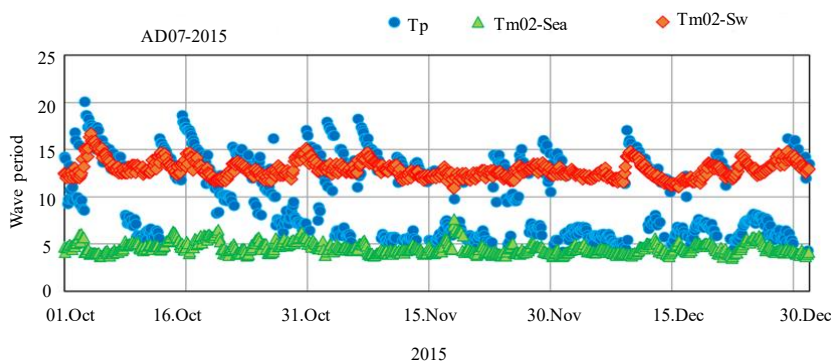


Figure 4. The sea & swell mean wave period are superposed on Tp during post-monsoon 2015.

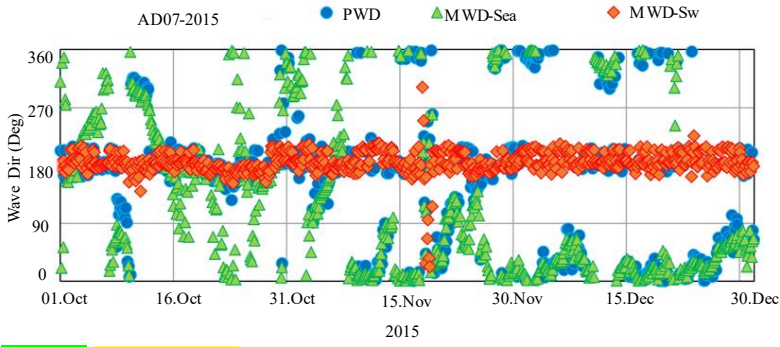


Figure 5. The sea & swell mean wave directions are superposed on peak wave direction during post-monsoon 2015.

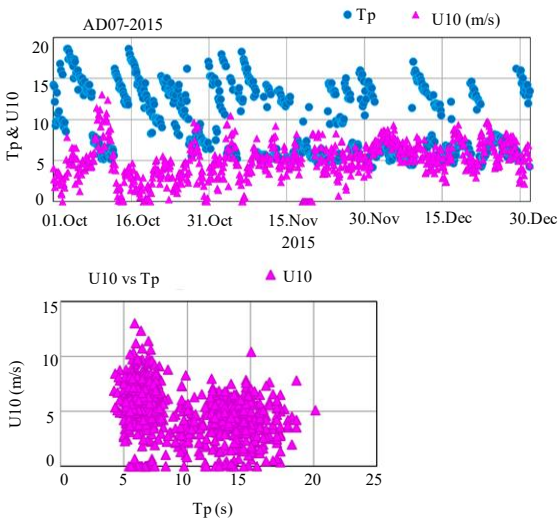


Figure 6. (left) The wind speed at 10m height is superposed on peak period T_p (right) T_p vs U_{10} during post-monsoon 2015.

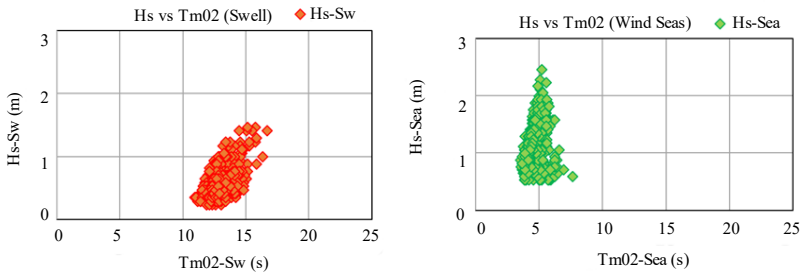


Figure 7. T_{m02} vs H_s for (left) swells & (right) wind seas

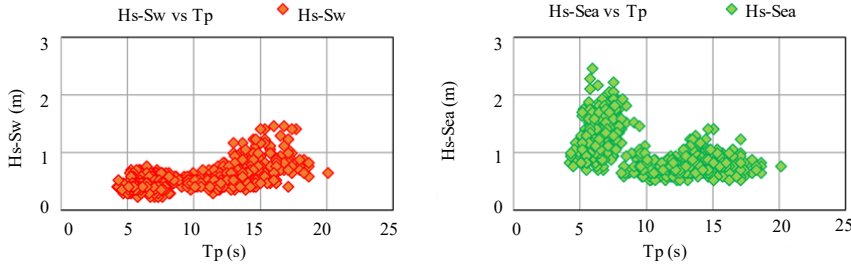


Figure 8. Tp vs Hs for (left) swells & (right) wind seas

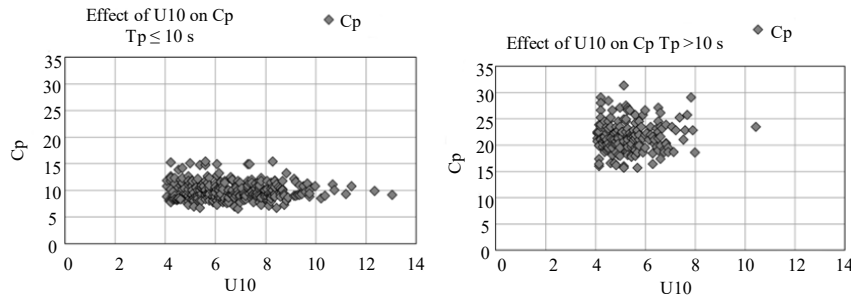


Figure 9. U10 vs wave celerity for (left) $T_p \leq 10$ s & (right) $T_p > 10$ s.

The components of Hs are plotted against the peak wave period T_p against Hs-swell (left) and Hs-seas (right) in the Figure .8. T_p extends from 4 to 20 s in both the cases. But the wave height ranges are high for wind seas (Hs-sea) for both $T_p \leq 10$ s and $T_p > 10$ s than the Hs-swells.

The wave celerity (phase speed, calculated based on T_p , dominant wave period) $C_p (=gT_p/2\pi)$ is plotted against wind speed U_{10} for $T_p \leq 10$ s on the left and $T_p > 10$ s on the right in Fig. 9. C_p is proportional to T_p and hence, C_p varied between 5 to 15 m/s for $T_p \leq 10$ s and between 15 to 30 m/s for $T_p > 10$ s. The corresponding U_{10} varied from 4 to 13 m/s for $T_p \leq 10$ s and 4 to 8 m/s except for peak instant (10.4 m/s) for $T_p > 10$ s.

The friction velocity u_* is plotted against U_{10} for $T_p \leq 10$ s on the left and $T_p > 10$ s on the right in Fig. 10. Friction velocity is proportional to C_d , drag coefficient. In this paper, C_d is kept constant up to $U_{10} < 11$ m/s and linearly varied based on $U_{10} > 11$ m/s as per Large and Pond (1981) [8].

$$C_d = 1.2 \times 10^{-3} \text{ for } U_{10} < 11 \text{ m/s \&}$$

$$C_d = (0.49 + 0.065 U_{10}) \times 10^{-3} \text{ for } 11 < U_{10} < 25 \text{ m/s} \quad (1)$$

$$\text{Wind-stress } \tau = \rho C_d (U_{10})^2 \quad (2)$$

$$\text{Friction velocity } u_* = \sqrt{\frac{\tau}{\rho}} \quad (3)$$

Hence, for $T_p > 10$ s, with U_{10} less than 11 m/s, C_d was constant at 0.0012 and u_* varied between 0.1 to 0.3 m/s except one peak instance of 0.36 m/s. Hence, a straight line is obtained with linear variation between u_* vs U_{10} . For $T_p \leq 10$ s, few instances of $U_{10} \geq 11$ m/s, changed the trend of the linear relationship for u_* in the 0.39 to 0.47 m/s.

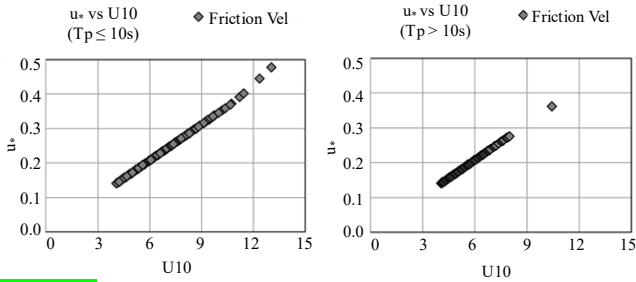


Figure 10. U10 vs friction velocity u_* for (left) $T_p \leq 10s$ & (right) $T_p > 10s$.

The wave steepness and wave age are derived based on the following. With significant wave properties, wave steepness and wave age are defined as

$$\epsilon = \frac{H_s}{L_p} = \frac{2\pi H_s}{gT_p^2} \quad (4)$$

$$\beta = \frac{C_p}{U_{10}} = \frac{gT_p}{2\pi U_{10}} \quad (5)$$

$$\beta_* = \frac{C_p}{u_*} = \frac{gT_p}{2\pi u_*} \quad (6)$$

where, H_s is the significant wave height, L_p is the wave length corresponding to the peak wave period T_p , g is acceleration due to gravity. C_p is the phase speed of waves, u_* is the surface wind frictional velocity. ϵ is wave steepness and β is wave age while β_* corresponds to wave age with respect to friction velocity u_* .

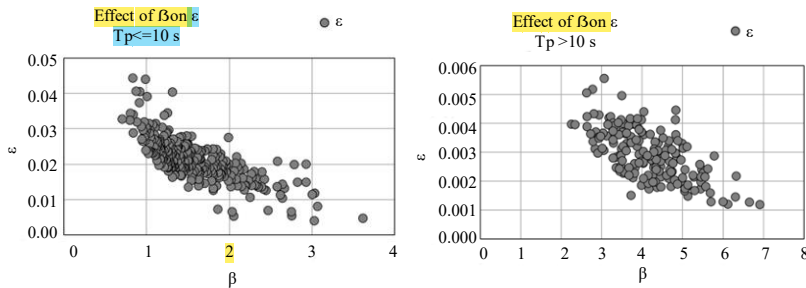


Figure 11. Variation of wave steepness (ϵ) with wave age (β) (left) $T_p \leq 10s$ & (right) $T_p > 10s$.

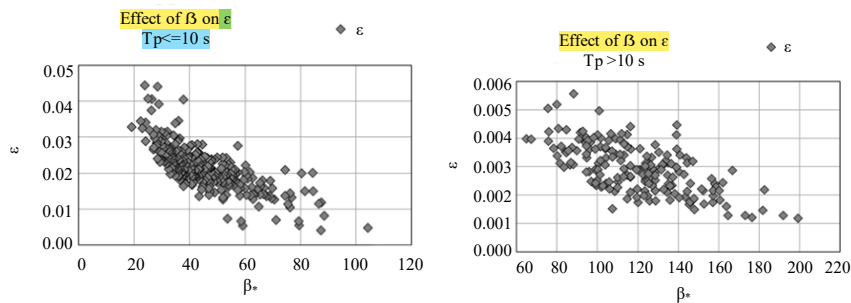


Figure 12. Variation of wave steepness (ϵ) with wave age (β_*) (left) $T_p \leq 10s$ & (right) $T_p > 10s$.

Table 1. Classification of Swells based on wave steepness

S n.	Steepness	Age of swells	Total = 736 (Post-monsoon-OND) U10 ≥ 4 m/s = 496 (67.4 %)		
			Tp ≤10 s 311 (62.7 %)	Tp >10 s 185 (37.3 %)	Total (496)
1	Less than 0.004	Old swells	Nil	87 %	32.5 %
2	0.004 – 0.01	Mature swells	2.9 %	13 %	6.7 %
3	0.01 – 0.025	Young swells	74.3 %	Nil	46.6 %
4	Greater than 0.025	Wind Seas	22.8 %	Nil	14.3 %

The types of swells at AD07 location during post-monsoon season, are classified into young, mature and old swells based on significant wave steepness—a measure of relative wave age (Thompson et al., 1984) in Table 1[14].

The total number of data points for October, November & December (OND) 2015 during post-monsoon were 736 at 3 hourly intervals. Out of which, 32.6% points were removed (U10 < 4 m/s). The data points with U10 > 4 m/s (496) are used for analysis (Figure 13) and consists of 37.3% (185 points) with Tp > 10 s and 62.7 % (311 points) as Tp ≤ 10 s. The long period waves with Tp > 10 s consists of 87% old swells and 13% mature swells. Short period waves with Tp ≤ 10 s consists of 3% mature swells, 74 % young swells and 23% wind seas.

Overall, from the 496 data points analysed with U10 ≥ 4 m/s; it is found that 32.5 % are old swells, 6.7 %, are mature swells, 46.6 % are young swells and only 14.3 % are wind seas in the deep waters of the Central Arabian Sea at AD07 buoy location during post-monsoon, as shown in Figure 14. As there were no cyclones that influenced AD07 during this period (Chapala & Megh were away from AD07 and had landfall on Gulf coast, no impact at AD07) the swells predominantly are from the SIO.

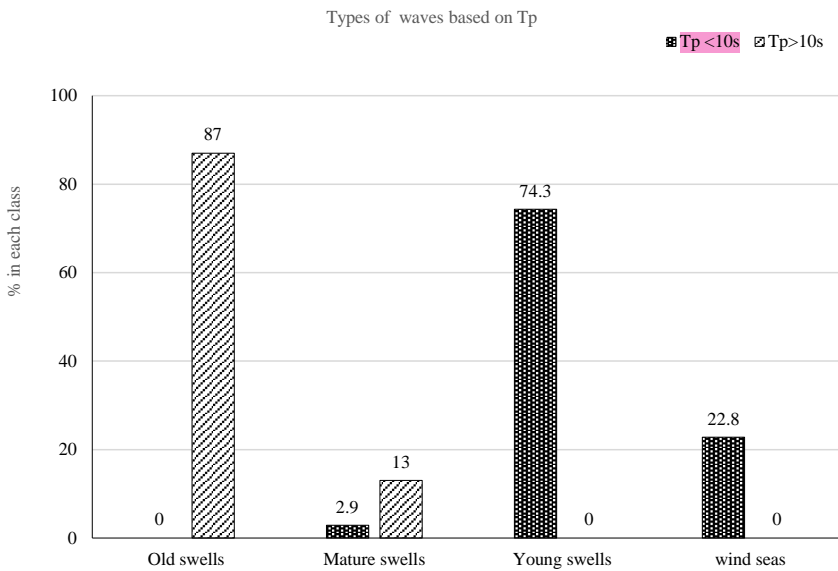


Figure 13. Wave type classification based on wave steepness and Tp at 10s.

Types of waves during post monsoon at AD 07



Figure 14. Wave type classification based on wave steepness for all Tp.

EMPIRICAL RELATIONSHIPS USING BUOY DATA

Relationship between ϵ - β for Wind Seas

For wind waves in local equilibrium with the wind, Toba (1972) [16]. proposed the well-known “3/2-power law” show as:

$$H_* = BT_*^{3/2} \quad (7)$$

where, $H_* = gH_S/u_*^2$, $T_* = gT_S/u_*$ and $B=0.062$. The law indicates that, in wind waves free of swells, the characteristic wave height and wave period are not independent of each other due to the coupling between wind and wind waves, but comply with Eq. (7).

Multiplying Eq. (7) by $2\pi u_*^2/g^2 T_p^2$ and using $T_S = 0.91T_p$ and $C_d = (u_*/U_{10})^2$, where C_d is the drag coefficient, Eq. (7) can be rewritten as

$$\epsilon = 0.135C_d^{1/4}\beta^{-1/2} \quad (8)$$

$$\epsilon = 0.135\beta_*^{-1/2} \quad (9)$$

$$\beta_* = C_p/u_* \quad (10)$$

Eq. (8) shows that wave steepness ϵ is a function of both wave age β and drag coefficient C_d . It suggests that wave steepness ϵ decreases with increasing wave age β , and that for a given wave age, the larger drag coefficient leads to the larger wave steepness. Eq. (9) states that wave steepness ϵ depends only on wave age β_* as defined by Eq. (10) in terms of friction velocity. According to Amorocho and De Vries (1980) [1], the onset of wave breakers starts at about 7 m/s and the saturation of wave breakers occurs at approximately 25 m/s, at which the wind drags sea foam and spray rather than the true sea surface waves [2]. The present paper focuses on the case of wind waves in deep water without the saturation of wave breakers. So, data in the available datasets are selected according to Wind speed condition: $4 \text{ m/s} \leq U_{10} \leq 25 \text{ m/s}$; Deep water condition: $L_p \leq 4d$, where d is water depth. The ϵ - β relationship derived from the 3/2-power law was strongly supported by the observational data of Liu Bin et. Al. (2007) [9].

Not for Distribution, Uploading, or Publication on Any Other Website (or Online Platform)
 Except Journals Official Website.

Galley Proof for Author's Review and Approval Only.

The available empirical relationship on wave steepness and wave age based on the 3/2 power law for wind seas is compared with the present AD07 data and found to follow the trend with an offset of 0.003. A similar relationship with a new coefficient for AD07 deepwater case during post-monsoon season (0.151) has been derived as against 0.135 that was fitted for the observational data of Liu Bin et. Al. (2007) [9]. Figure 15 shows the ϵ - β relationship derived from the 3/2-power law. It is shown that wave steepness increases with drag coefficient and decreases with increasing wave age β .

Relationship between Hs and Tp for Wind Seas

The empirical relationship developed between the non-dimensional wave height and wave period in the shallow waters of AS (Rashmi et. al. 2013) is compared with present data in deep waters at AD07 [11].

For shallow waters of Arabian Sea (Rashmi et. al. 2013) [11],

$$\frac{gH_s(sea)}{U_{10}^2} = 0.0085 \left(\frac{gT_p(sea)}{U} \right)^{1.515} \tag{11}$$

A similar relationship with modified coefficient 0.0108 (deep waters) as against 0.0085 (Coastal region) is derived for present data at AD07 for post-monsoon season as shown in Fig. 16 is given by

For deep waters of Arabian Sea at AD07

$$\frac{gH_s(sea)}{U_{10}^2} = 0.0108 \left(\frac{gT_p(sea)}{U} \right)^{1.515} \tag{12}$$

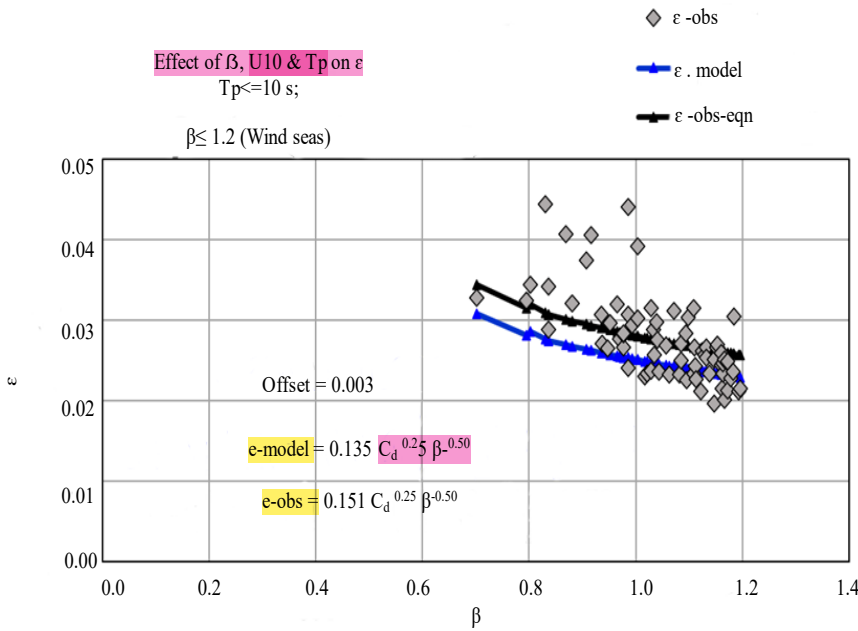


Figure 15. Comparison of Wave steepness (ϵ) and wave age (β) relationship based on 3/2 power law [9], with that of the deep waters at AD07 for wind seas

Galley Proof for Author's Review and Approval Only.

Not for Distribution, Uploading, or Publication on Any Other Website (or Online Platform) Except Journals Official Website.

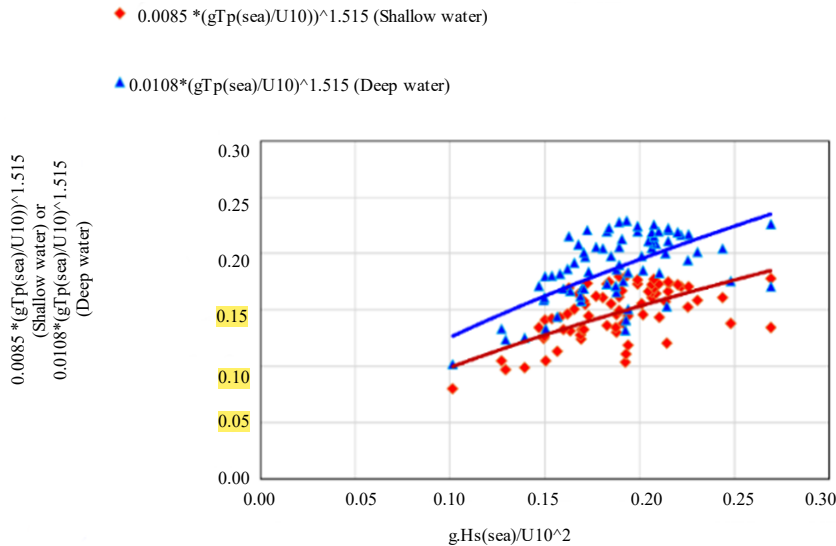


Figure 16. Comparison of relationship between nondimensional wave height and non-dimensional peak period for coastal waters (Rashmi et. al. 2013) [11], with that of the deep waters at AD07 for wind seas

CONCLUSIONS

1. Based on the measurements at AD07 buoy location in the central Arabian Sea in deep waters, the wave characteristics during post-monsoon season (OND) in the year 2015 for wind speeds greater than 4 m/s are segregated into different categories based on the wave steepness as 32.5 % old swells, 6.7 % mature swells, 46.6 % young swells and only 14.3 % wind seas.
2. As there were no cyclones that influenced AD07 during this period (Chapala & Megh were away from AD07 and had landfall on Gulf coast, no impact at AD07) the swells predominantly are from the SIO.
3. The available empirical relationship on wave steepness and wave age based on the $3/2$ power law is compared with the present AD07 data and found to follow the trend with an offset of 0.003. A similar relationship with a new coefficient for AD07 deepwater case during post-monsoon season (0.151) has been derived as against 0.135 that was fitted for the observational data of Liu Bin et. Al. (2007) [9].
4. The empirical relationship between the non-dimensional wave height and wave period in the shallow waters of AS derived by Rashmi et. al. 2013, is compared with present AD07 data in deep waters [11]. A similar relationship with modified coefficient 0.0108 (for deep water case) as against 0.0085 (Coastal waters) is derived for the post-monsoon season at AD07.

Acknowledgements

The authors express their sincere gratitude to Ministry of Earth Sciences for providing the opportunity to work on this project. We sincerely thank Dr. R. Balaji, Director, NIOT, for his support and encouragement to conduct this work. We acknowledge the efforts of all the staff members of the Ocean Observation Systems Group of NIOT who are behind the field work for providing the measured data and the VMC group for their ship time.

REFERENCES

1. Amoroch, J. and J. J. DeVries, 1980. A new evaluation of the wind stress coefficient over water surfaces. J. Geo phys. Res. 85(C1): 433-442.

2. Banner, M. L., W. Chen, E. J. Walsh, J. B. Jensen, S. Lee and C. Fandry, 1999. The Southern Ocean Waves Experiment. Part 1: Overview and mean results. *J. Phys. Oceanogr.* 29: 2 130-2 145.
3. Garratt, J. R., 1977. Review of drag coefficients over oceans and continents. *Mon. Wea. Rev.* 105: 915-929.
4. Geernaert, G. L., K. B. Katsaros and K. Richter, 1986. Variations of the drag coefficient and its dependence on sea state. *J. Geophys. Res.* 91: 7 667-7 679.
5. Guan, C. L. and Q. Sun, 2002. Analytically derived wind wave growth relationships. *China Ocean Engineering* 16(3): 359-368.
6. Guan, C. L. and L. A. Xie, 2004. On the linear parameterization of drag coefficient over sea surface. *J. Phys. Oceanogr.* 34: 2847-2851.
7. Hou, Y. J. and T. Wang, 1993. Characteristic parameters of the wind wave spectrum. *Oceanologia et Limnologia Sinica* 24(2): 126-131. (in Chinese).
8. Large, W. G., & Pond, S. (1981). Open Ocean Momentum Flux Measurements in Moderate to Strong Winds. *Journal of Physical Oceanography*, 11(3), 324–336.
9. Liu Bin, Ding Yun, Guan Changlong (2007). A relationship between wave steepness and wave age for wind waves in deep water, *Chinese Journal of Oceanology and Limnology*, Vol. 25 No. 1, P. 36-41, 2007 DOI: 10.1007/s00343-007-0036-6.
10. Remya, P. G., S. Vishnu, B. PraveenKumar, T. M. Balakrishnan Nair, and B. Rohith (2016), Teleconnection between the North Indian Ocean high swell events and meteorological conditions over the Southern Indian Ocean, *J. Geophys. Res. Oceans*, 121,7476–7494, doi:10.1002/2016JC011723.
11. Rashmi, R., V. M. Aboobacker, P. Vethamony and M. P. John (2013). Co-existence of wind seas and swells along the west coast of India during non-monsoon season, *OceanSci.*,9, 2013, pp. 281–292. doi:10.5194/os-9-281-2013.
12. Sanil Kumar, V., C. Sajiv Philip and T. N. Balakrishnan Nair (2010). Waves in shallow water off west coast of India during the onset of summer monsoon, *Ann.Geophys.*,28, 2010., pp. 817–824.
13. Smith, S. D., 1980. Wind stress and heat flux over the ocean in gale force winds. *J. Phys. Oceanogr.* 10: 709-726.
14. Thompson, W. C., Nelson, A. R., and Sedivy, D. G.: Wave group anatomy. Proceedings of 19th conference on Coastal Engineering, Vol. I, American Societ of Civil Engineers, 661–677, 1984.
15. Toba, Y., 1972. Local balance of in the air-sea boundary processes, I: On the growth process of wind waves. *J. Oceanogr. Soc. Japan* 28: 109-120.
16. Toba, Y., 1998. Wind-forced strong wave interactions and quasi-local equilibrium between wind and wind sea with the friction velocity proportionality. In: W. Perrie ed. *Nonlinear Ocean Waves (Advances in Fluid Mechanics, Vol. 17, Series editor: M. Rahman)*. Computational Mechanics Publications, Southampton and Boston. p. 1-59.
17. Wang, B. X., 1990. An investigation on the δ - β relationship of ocean waves. *J. Ocean Univ. Qingdao* 20(3): 1-9. (in Chinese).
18. Wen, S. C., 1962. *Ocean Wave Theory*, Shandong People’s Press, Jinan, China. p. 224-265. (in Chinese).
19. Wu, J., 1980. Wind-stress coefficients over sea surface near neutral conditions—a revisit. *J. Phys. Oceanogr.* 10: 727-740.
20. Yelland, M. J. and P. K. Taylor, 1996. Wind stress measurements from the open ocean. *J. Phys. Oceanogr.* 26: 541-558.

Not for Distribution, Uploading, or Publication on Any Other Website (or Online Platform)
Except Journals Official Website.

Galley Proof for Author's Review and Approval Only.